(3) Bueche, F. *J. Chem. Phys.* **1956**, *25*, 599.
(4) Graessley, W. W. *J. Chem. Phys.* **1965**, *43*, 2696; **1967**, *47*, 1942; **1971**, *54*, 5143.
(5) de Gennes, P.-G. *J. Chem. Phys.* **1971**, *55*, 572.
(6) de Gennes, P.-G. "Scaling Concepts in Polymer Physics"; Cornell University Press: Ithaca, NY, 1979.
(7) Doi, M.; Edwards, S. F. *J. Chem. Soc., Faraday Trans. 2* **1978**, *74*, 1789; **1978**, *74*, 1802; **1978**, *74*, 1818; **1979**, *75*, 38.
(8) Doi, M. *J. Polym. Sci., Polym. Phys. Ed.* **1980**, *18*, 1005; **1980**, *18*, 1981.
(9) Evans, K. E.; Edwards, S. F. *J. Chem. Soc., Faraday Trans. 2* **1981**, *77*, 1891; **1981**, *77*, 1913; **1981**, *77*, 1929.
(10) Hansen, D. R.; Williams, M. C.; Shen, M. *Macromolecules* **1976**, *9*, 345. Hong, S. D.; Hansen, D. R.; Williams, M. C.; Shen, M. *J. Polym. Sci., Polym. Phys. Ed.* **1977**, *15*, 1869.
(11) Klein, J. *Macromolecules* **1978**, *11*, 852.
(12) Graessley, W. W. *Adv. Polym. Sci.* **1982**, *47*.
(13) Doi, M. *J. Polym. Sci., Polym. Phys. Ed.* **1983**, *21*, 667.
(14) Ninomiya, K. *J. Colloid Sci.* **1959**, *14*, 49. Ninomiya, K.; Ferry, J. D. *Ibid.* **1963**, *18*, 421.
(15) Masuda, T.; Kitagawa, K.; Inoue, T.; Onogi, S. *Macromolecules* **1970**, *2*, 116.
(16) Bogue, D. G.; Masuda, T.; Einaga, Y.; Onogi, S. *Polym. J.* **1970**, *1*, 563.
(17) Prest, W. M.; Porter, R. S. *Polym. J.* **1973**, *4*, 154. Prest, W. M. *Ibid.* **1973**, *4*, 163.
(18) Kurata, M.; Osaki, K.; Einaga, Y. *J. Polym. Sci., Polym. Phys. Ed.* **1974**, *12*, 849.
(19) Friedman, E. M.; Porter, R. S. *Trans. Soc. Rheol.* **1975**, *19*, 493.
(20) Soong, D. S.; Shen, M.; Hong, S. D. *J. Rheol.* **1979**, *23*, 301. Soong, D. S.; Shyu, S. S.; Shen, M.; Hong, S. D.; Moacanin, J. *J. Appl. Phys.* **1979**, *50*, 6007. Soong, D. S.; Shyu, S. S.; Shen, M. *J. Macromol. Sci., Phys.* **1981**, *B19*, 49.
(21) Kinouchi, M.; Takahashi, M.; Masuda, T.; Onogi, S. *J. Soc. Rheol. Jpn.* **1974**, *4*, 25.
(22) Liu, T. Y.; Soong, D. S., Williams, M. C. *J. Rheol.* **1983**, *27*, 7.
(23) Graessley, W. W. *J. Polym. Sci., Polym. Phys. Ed.* **1980**, *18*, 27.
(24) Kurata, M. *Macromolecules* **1984**, *17*, 895.
(25) Masuda, T.; Yoshimatsu, S.; Takahashi, M.; Onogi, S. *Polym. Prepr. Jpn.* **1983**, *32*(9), 2365.
(26) Markovitz, H. *J. Appl. Phys.* **1952**, *23*, 1070.
(27) Tschoegl, N. W. *Rheol. Acta* **1971**, *10*, 582.
(28) The observed M_{w1}^3 dependence (rather than $M_{w1}^{3.4}$) of τ_{12} (eq 5) implies that the tube renewal process is taking place essentially by the *pure* reptation of 1-chains without involving other mechanisms such as the contour length fluctuation, as suggested by Klein[11] and Graessley.[12] This is presumably because the tube renewal process is governed by the diffusion (not by the stress relaxation) of the tube forming 1-chains. In fact, observed molecular weight dependence of the (macroscopic) diffusion coefficient D_G ($\propto M^{-2}$)[29,30] was successfully accounted by the tube model incorporating only the *pure* reptation, while the $M^{3.4}$ dependence of η_0 was not. In other words, the mechanical relaxation of the 1-chain takes place by all the mechanisms releasing its constraints but its diffusion dominantly by reptation of the 1-chain.
(29) Klein, J. *Philos. Mag.* **1981**, *43*, 771.
(30) Leger, L.; Hervet, H.; Rondlez, F. *Macromolecules* **1981**, *14*, 1732.
(31) Osaki, K.; Nishizawa, K.; Kurata, M. *Macromolecules* **1982**, *15*, 1068.
(32) According to Doi,[13] $N^3N_e^{-1}[1 - 1.47(N_e/N)^{0.5}]^2$ is almost proportional to $N_e^{-1.4}N^{3.4}$ in the range $5 < N/N_e < 50$ and we obtain eq 10′ and 14a by putting $N_e \propto w_2^{-1}$.
(33) Strictly speaking, this replacement is only approximate because the cut-off time τ^* for the wedge spectrum in the transition zone for the 1-chain does not depend on w_2 while that τ_{11} for its box spectrum depends on w_2. However, the shift of τ_{11} is not large as shown in Figure 7, and we employ this approximation at present for simplicity.

Morphological and Viscoelastic Properties of Poly(styrene-*b*-butadiene-*b*-4-vinylpyridine) Three-Block Polymers of the ABC Type

Itaru Kudose and Tadao Kotaka*

Department of Macromolecular Science, Faculty of Science, Osaka University, Toyonaka, Osaka 560, Japan. *Received October 19, 1983*

ABSTRACT: A series of poly(styrene-*b*-butadiene-*b*-4-vinylpyridine) three-block (SBP) polymers of the ABC type, in which the composition was roughly *X*:1:1 with *X* varying from 1 to 8, were prepared. Their morphological and viscoelastic properties were compared with those of our previous samples having 1:*Y*:1 composition with *Y* varying from 1 to 4. The polymers were cast from $CHCl_3$ and from butyraldehyde (BA)/$CHCl_3$ (9/1 (v/v)) or tetrahydrofuran/methanol (4/1 or 9/1 (v/v)) mixtures (BA-system solvents). SBP samples having roughly 1:1:1 composition cast from $CHCl_3$ exhibited a "ball-in-a-box" structure, in which spherical poly(4-vinylpyridine) (P4VP) domains enclosed by polybutadiene (PB) shells were embedded in the polystyrene (PS) matrix phase. The size of the P4VP balls became progressively smaller with decreasing P4VP block length. The same samples with 1:1:1 composition cast from a BA-system solvent exhibited "three-layer-lamellar" morphology. With increasing *X*, the P4VP lamellae changed to cylinders and finally to spheres surrounded by PB shells, and the PS lamellae to the matrix. The specimens having P4VP spherical domains with PB shells exhibited only two viscoelastic relaxations corresponding to the glass transitions of the PB and PS phases. However, those having continuous P4VP (either lamellar or cylindrical) domains showed three transitions corresponding to the three phases. Probably, in the former, the mechanical excitations were absorbed and dissipated in the soft PB phase and not transmitted to the hard P4VP phase. However, in the latter, the P4VP phase forming continuous domains contributed to the mechanical loss.

Introduction

ABC three-block polymers[1-9] and their use as special function materials[1-3] have attracted much attention. Recently, work has been extended to explore three-component pentablock polymers of the BABCB type in search of more sophisticated applications.[10] In our previous publications,[6,7] we reported the synthesis, characterization, and morphological and mechanical properties of poly(styrene-*b*-butadiene-*b*-4-vinylpyridine) three-block polymers of the ABC type, which were referred to as SBP polymers. Although the morphology of microphase-separated structures in ABC three-block polymers[5-7] is in general more difficult to control than that in AB diblock copolymers,[11,12] we succeeded in developing two different types of unique morphology from an SBP polymer (coded as SBP-1 having approximately 1:1:1.3 volume composi-

0024-9297/84/2217-2325$01.50/0

tion) by choosing suitable casting solvents.[6-8] These SBP-1 specimens with different morphology exhibited different mechanical properties. We also examined two other SBP polymers coded as SBP-2 and -3, which had 1:*Y*:1 composition with a PB content *Y* of about 2 and 4, respectively.[6,7] Since then, we have prepared some more SBP polymers having *X*:1:1 composition (with PS content *X* varying from 1 to 8) and attempted to elucidate the relations between the composition and the morphological and viscoelastic properties of these SBP polymers.[8] In this article, we report the results obtained.

Experimental Section

Materials. Synthesis of the Block Polymers. The reagents used for the synthesis were purified and prepared by the methods recommended by Fetters[13] and by Fujimoto.[14] The details are described in our previous paper.[6] However, in this study, styrene (S) was purified by using di-*sec*-butylmagnesium[15] and not by brief purging with *sec*-butyllithium as done in the previous study.[6]

The polymerization of SBP (or SP) block polymers was carried out by a three-stage (or two-stage) sequential addition of styrene (S), butadiene (B), and 4-vinylpyridine (4VP) in benzene with *sec*-butyllithium as the primary initiator for S. At each stage, aliquots were taken to recover the PS precursor and SB intermediate to be used for a later characterization study. The polymerization of 4VP with polybutadienyl (or polystyryl) anions at the final step of the reaction was carried out at about 10 °C to prevent undesirable side reactions.[16] The details are described also in our previous paper.[6]

Since P4VP was insoluble in benzene, it was difficult to obtain block polymers with high P4VP content or long P4VP blocks by the present method. Hence, a few samples with high P4VP content were prepared, replacing the polymerization solvent, benzene, by tetrahydrofuran (THF) just before 4VP was introduced into the mixture at the final step.[8] The results on these P4VP-rich samples will be reported elsewhere.

A commercially available SBS sample (Kraton 1101, Shell Chemical Co.) was used as a reference. This sample had M_n = 95.1 × 10^3 and a PS content of 33% (w/w).

Film Preparation. Adequate casting solvents for SBP polymers were sought by solubility tests of SBP-1, -2, and -3 and SBS in a variety of pure solvents.[6,8] Among more than 30 solvents examined, $CHCl_3$, CH_2Cl_2, and a few other halogen-containing hydrocarbons were found to dissolve all the samples fairly well. From this group, we selected $CHCl_3$ as a casting solvent.[6] *n*-Butyraldehyde (BA) was unique in the sense that it dissolved SBP-1 (having the highest P4VP content among the four samples tested) better than SBP-3 and SBS. Thus, BA is a better solvent for P4VP blocks but a poor one for PB blocks.

Only a few pure solvents were found to be adequate for casting all SBP polymers examined in this study. Thus, we selected a variety of solvents, some of which were good for SB (S^{SB}) and some of which were good for only S (S^S), B (S^B), or P (S^P), to make their binary mixtures and tested the solubility of SBP polymers in the following combinations of binary solvents: S^{SB}/S^P, S^S/S^P, and S^B/S^P.[6-8]

The casting from a binary solvent required the following conditions. First of all, the polymer must be soluble in the binary solvent or should give a transparent solution, at least at the beginning. Second, the solvent composition should not change much so that the solution stays transparent during the entire stage of casting. Otherwise, no films having reproducible microdomain structure can be obtained.[7,8]

The results of the above test[6-8] showed that the binary mixtures butyraldehyde (BA)/$CHCl_3$ (9/1 (v/v)) and tetrahydrofuran (THF)/methanol (MeOH) (9/1 or 4/1 (v/v)) met the above criteria and were adequate for casting the SBP polymers to obtain films with reproducible morphology. For BA/$CHCl_3$ mixtures, BA is much less volatile than $CHCl_3$ (the vapor pressure at 25 °C is 118 mmHg for BA vs. 194.8 mmHg for $CHCl_3$). Therefore, $CHCl_3$ was lost in an early stage of casting, and the microdomain formation proceeded essentially in BA. On the other hand, for THF/MeOH mixtures, the solvent composition was found to remain in the 9/1 to 4/1 (v/v) range during the entire stage of casting.[7] The details of these tests were described elsewhere.[6,7]

The reported solubility parameter values[17] [in (cal $cm^{-3})^{1/2}$] of the component homopolymers are 8.2 for PB, 9.1 for PS, and 10–12 for P4VP, and those of the solvents are 9.3 for $CHCl_3$, 9.5 for BA, 9.9 for THF, and 14.5 for MeOH. Therefore, $CHCl_3$ is good for PS and PB blocks but poor for P4VP blocks. The two binary mixtures are somewhat better for P4VP blocks but poor for PB blocks. The former type solvents are called the $CHCl_3$ system and the latter the BA system.[6-8]

In most cases, SBP polymers were cast from 3% (w/v) solutions on a flat-bottom Teflon cell. The solvent was allowed to evaporate slowly at room temperature over a period of 7–10 days. Films were further dried at room temperature under a vacuum of about 10^{-3} torr for 3 more days. The film thickness was 0.2–0.5 mm.

Methods. Molecular Characterization. Number-average molecular weights M_n of the polymer samples were determined by osmometry in $CHCl_3$ at 25 °C with a Wescan recording osmometer (Wescan Instruments, Model 231) and membrane filter RC-52 (Astec Co.) of 10 μm pore size. The PS and P4VP content of each sample was determined by UV absorbance in $CHCl_3$, using a Jasco automatic recording spectrometer (Nihon Bunko Co., Model UNIDEC-5A).

The M_n and molecular weight distributions of the PS precursors and SB intermediates were determined by a gel permeation chromatograph (GPC; Toyo Soda Mfg. Co., Ltd., Model HLC-801A) equipped with a built-in refractometer, a UV detector (Toyo Soda, UV-8), and a low-angle laser light scattering photometer (Toyo Soda, LS-8) connected in series. With $CHCl_3$ as the eluent, the GPC was operated at 40 °C and a flow rate of about 1.0 mL min^{-1}. The polymer concentrations were between 0.03 and 0.06% (w/v). Commercially available narrow-distribution PS samples (Pressure Chemical Co. and Toyo Soda) were used for calibration.

None of the block polymers containing P4VP blocks were analyzable by GPC, because they were adsorbed on the cross-linked PS gels. Thus, their heterogeneity was examined by ultracentrifugation on $CHCl_3$ solutions at 20 °C. A Beckman-Spinco analytical ultracentrifuge (Model E) equipped with a schlieren optical system was used. The polymer concentrations were 0.2% (w/v). The ultracentrifuge was operated usually at a speed between 40 000 and 50 000 rpm.[6,8]

Morphological Observation. Electron micrographs were taken by Mr. Kenji Yoshimura at Toray Research Center. In most cases, as-cast films were trimmed and exposed to OsO_4 vapor over a 1% aqueous solution at room temperature for about 4–7 days. The stained specimens were microtomed normal to the film surface to obtain ultrathin sections 40–60 nm thick. A Hitachi transmission electron microscope (Model HV-10) was used at an accelerating voltage of 75 kV.

Mechanical and Thermal Properties. Dynamic mechanical properties were measured by a Rheovibron DDV-IIC (Toyo-Baldwin Co.) at a frequency of 110 Hz and a heating rate of about 1 K min^{-1}. Thermal properties were measured by a differential scanning calorimeter (DSC; Rigaku Denki Co., Model 8055) over a temperature range from 150 to 450 K at a heating rate of 10 K min^{-1}. In most cases, samples of 15–30 mg were used.

Results

Molecular Characterization. Table I summarizes the characteristics of the SBP polymers and SP diblock copolymers used in this study. For convenience, three previously prepared samples[6] are also listed in this table. The microstructure of PB sequences was determined by the infrared spectroscopy proposed by Morero et al.[18] A typical result was 10% 1,2-vinyl, 39% cis-1,4, and 51% trans-1,4 configurations, which agreed with literature values for homopolybutadienes prepared by a similar anionic polymerization method.[19] The osmometry, UV absorption measurements, GPC, and ultracentrifugation velocity experiments all confirmed that these samples have a well-defined linear ABC architecture and consist of blocks fairly narrow in molecular weight distribution.[6-8]

The M_n values from Table I and the reported bulk density values of 1.05, 0.89, and 1.114 for PS, PB,[17] and P4VP,[20] respectively, were used to estimate the volume fraction of the components in each sample. Figure 1 shows

Table I
Characteristics of the Polymer Samples[a,b]

code	$10^{-3}M_n$				vol comp		
	M_n^S $(M_w/M_n)^S$	M_n^B	M_n^P	M_{nt}	ϕ_S	ϕ_B	ϕ_P
SBP Three-Block Polymers							
SBP-1	20.2 (1.06)	22.0	32.3	74.5	0.26	0.34	0.40
SBP-2	23.3 (1.04)	45.2	22.3	90.8	0.24	0.55	0.22
SBP-3	13.0 (1.06)	76.7	22.8	112.5	0.10	0.72	0.17
SBP-10	30.1 (1.08)	14.3	28.5	72.9	0.41	0.23	0.36
SBP-11	23.3 (1.08)	14.2	19.7	57.2	0.40	0.29	0.32
SBP-12	13.3 (1.06)	15.6	24.2	53.0	0.24	0.34	0.42
SBP-13	29.9 (1.06)	12.7	9.8	52.4	0.55	0.28	0.17
SBP-14	44.0 (1.05)	4.9	5.4	54.3	0.80	0.11	0.09
SP Diblock Copolymers							
SP-1	54.0 (1.09)		53.7	107.7	0.52		0.48
SP-3	55.3 (1.06)		10.9	66.2	0.84		0.16

[a] $(M_w/M_n)^S$ values for PS precursors; M_{nt} is the total number-average molecular weight. [b] For the weight fractions, $x_S:x_B:x_P = M_n^S:M_n^B:M_n^P$, while for the volume fractions, $\phi_S:\phi_B:\phi_P = M_n^S/\rho_S:M_n^B/\rho_B:M_n^P/\rho_P$ with bulk densities $\rho_S = 1.05$, $\rho_B = 0.89$, and $\rho_P = 1.114$ g cm^{-3}.

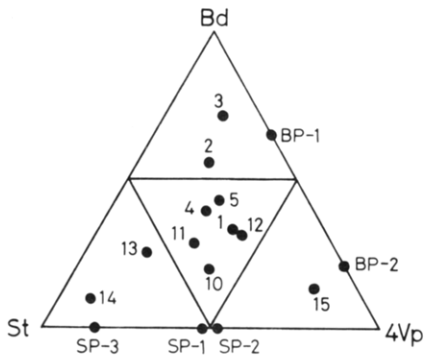

Figure 1. Volume composition diagram for the SBP and SP polymers used in this study.

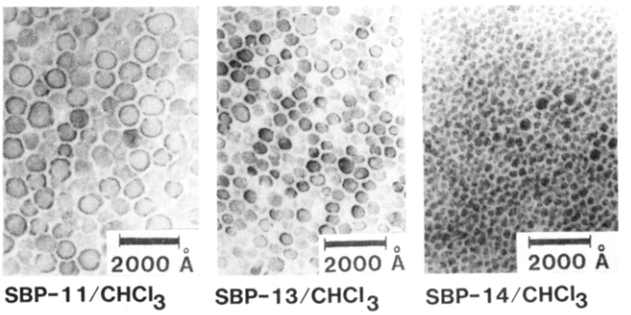

Figure 2. Electron micrographs of SBP-11, SBP-13, and SBP-14 as-cast specimens from $CHCl_3$.

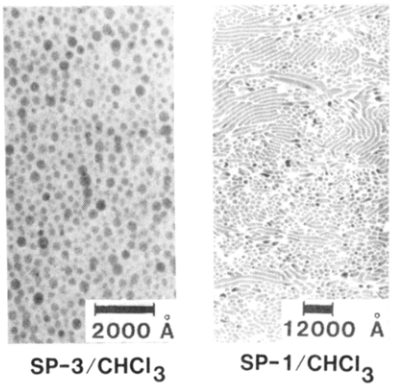

Figure 3. Electron micrographs of SP-1 and SP-3 as-cast specimens from $CHCl_3$.

the results on a traiangular composition diagram. This diagram also shows a few other samples not discussed in this study. The apexes, St, Bd, and 4Vp, correspond to the homopolymers, PS, PB, and P4VP, respectively, and the three sides to SB, BP, and SP diblock copolymers. The numberical data are also listed in Table I.

Morphology Observation. The casting solvents used may be classified into two categories according to the type of the microphase-separated structure formed in SBP-1 specimens.[6,7] The SBP-1 sample cast from $CHCl_3$ gave a specimen having gray circular domains surrounded by black domains and further by a light continuous matrix. Since OsO_4 selectively reacts with PB olefinic bonds and less strongly with nitrogen atoms in pyridine rings, we assigned the black regions to PB domains, the gray regions to P4VP domains, and the light matrix to the PS phase. Since two ultrathin sections cut perpendicular to each other and also to the film surface gave essentially identical micrographs, we concluded[6] that in the $CHCl_3$-cast SBP-1 specimen, spherical P4VP microdomains were surrounded by PB segments and sat in a continuous PS matrix (which looked like stacked boxes). We called this structure "ball-in-a-box" morphology. Incidentally, the calculated volume ration of the components in the "ball-in-a-box" structure (assuming that observed radii of the circles respresnt those of the spheres in the specimen) was comparable with the SBP composition in the polymer.[6]

On the other hand, an SBP-1 specimen cast from BA/$CHCl_3$ (9/1 (v/v)) and THF/MeOH (4/1 or 9/1 (v/v)) mixtures exhibited what we called a "three-layer-lamellar" structure, in which light, black, and gray continuous lamellae (corresponding to the SBP components, respectively) appeared alternately in the order ...SBP–PBS–SBP...[6,7] The thickness of the lamellae was approximately proportional to the SBP composition. However, a close examination of the micrographs of specimens cast from THF/MeOH mixtures showed that the PB phase forms not perfect lamellae but discontinuous domains.[6-8]

(a) Specimens Cast from $CHCl_3$. We have already reported[6] the changes in morphology of SBP-1, -2, and -3 samples having roughly 1:*Y*:1 composition with an increase in PB content *Y*. The increase in *Y* led to a disorganized "ball-in-a-box" structure, in which P4VP blocks still formed spherical domains but PS boxes were disrupted and became irregularly dispersed in the PB matrix phase.

Figure 2 shows electron micrographs for $CHCl_3$-cast specimens of SBP-11, -13, and -14, which had nearly the same molecular weight and *X*:1:1 composition with PS content *X* equal to 1.33 (40% (v/v)), 2 (55% (v/v)), and 8 (80% (v/v)), respectively. In these specimens, the size

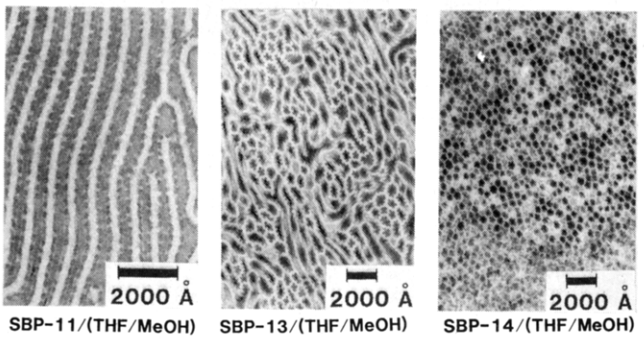

Figure 4. Electron micrographs of SBP-11, SBP-13, and SBP-14 sepcimens cast from a THF/MeOH 4/1 (v/v) mixture.

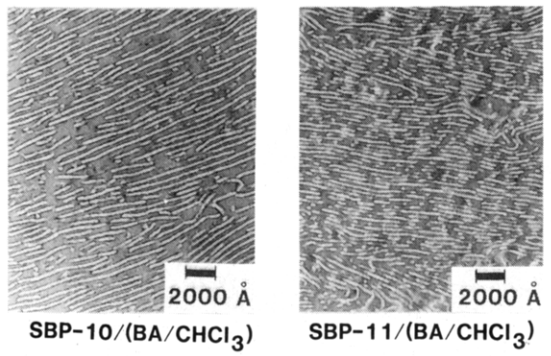

Figure 5. Electron micrographs of SBP-10 and SBP-11 specimens cast from a 9/1 BA/$CHCl_3$ mixture.

of P4VP spheres successively decreased with increasing X or decreasing P4VP block length, M_n^P.

For comparison, Figure 3 shows micrographs of SP-1 and -3 specimens cast from $CHCl_3$. Interestingly, the SP-1 sample with 1:1 composition exhibits a morphology consisting of gray P4VP cylinders or spheres embedded in a light PS matrix. For a 1:1 diblock copolymer, an alternating lamellar structure is known to be a more common morphology.[11,12]

(b) Specimens Cast from BA Systems. The SBP-1 sample cast from a BA/$CHCl_3$ mixture showed a regular "three-layer-lamellar" morphology. The SBP-2 and -3 samples cast from the same mixture exhibited highly irregular structures, in which irregular PS and P4VP domains were intermixed with the PB matrix phase.[6,7]

Figure 4 shows electron micrographs for THF/MeOH (4/1 (v/v)) cast specimens of the SBP-11, -13, and -14 samples. In these specimens, their morphology changes from the "three-layer-lamellar" type to that in which PS blocks form a matrix phase and P4VP blocks form cylindrical or spherical domains surrounded by cylindrical or spherical PB domains. The domain morphology of an ultrathin section cut perpendicular to these cylinders looked like a "sunflower". Figure 5 shows micrographs of BA/$CHCl_3$ (9/1) cast SBP-10 and -11 specimens. They exhibit a mixture of regular and disorganized "three-layer-lamellar" structures. Figure 6 shows micrographs of SP-1 and -3 samples cast from BA/$CHCl_3$ (9/1) and THF/MeOH (9/1) mixtures, respectively. In the SP-3 specimen, we observe a structure of P4VP spheres/PS matrix type, as in the $CHCl_3$-cast SP-3 specimen. However, in the SP-1 specimen, we observe mixed PS spherical and cylindrical domains embedded in the P4VP matrix. A phase inversion occurred in the SP-1 sample with the change in casting solvents from $CHCl_3$ to the BA/$CHCl_3$ mixture.

Dynamic Viscoelastic Properties. Figure 7 shows the temperature dependence of the tensile storage E' and loss

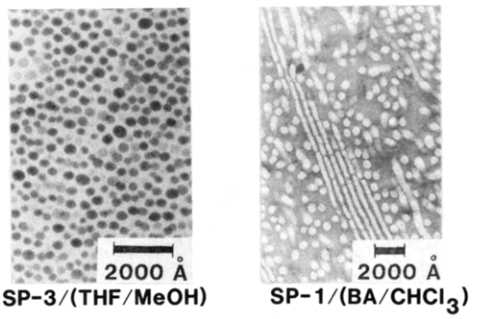

Figure 6. Electron micrographs of SP-1 specimen cast from a 9/1 BA/$CHCl_3$ mixture (right) and SP-3 specimen cast from a 9/1 THF/MeOH mixture (left).

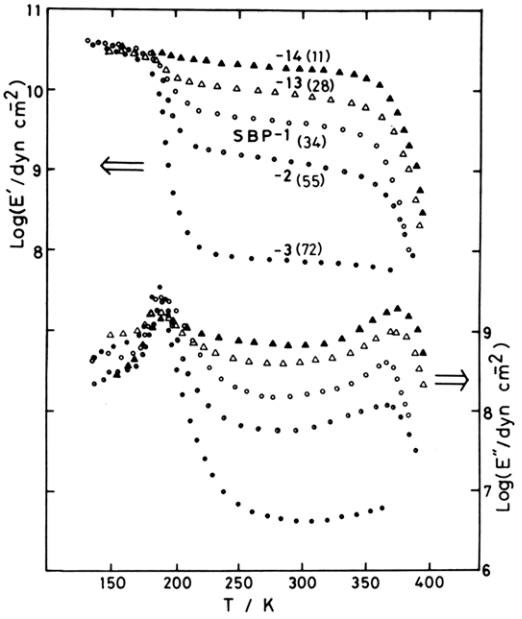

Figure 7. Temperature dependence of E' and E'' at 110 Hz of five SBP samples cast from $CHCl_3$.

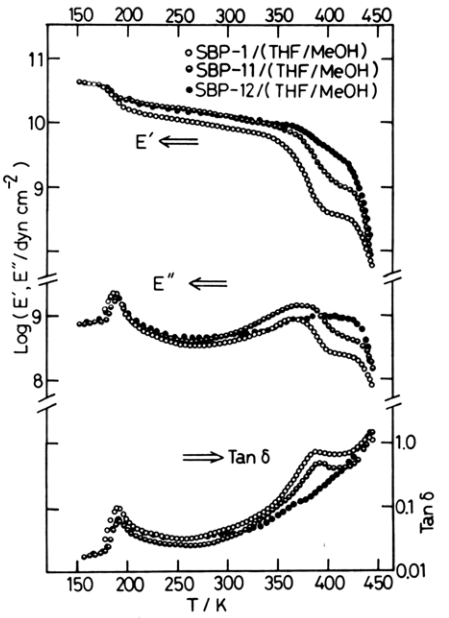

Figure 8. Temperature dependence of E', E'', and tan δ at 110 Hz of SBP-1, SBP-11, and SBP-12 specimens cast from a 4/1 THF/MeOH mixture.

E'' moduli for $CHCl_3$-cast SBP polymers. For comparison, our previous data on $CHCl_3$-cast SBP-1, -2, and -3 specimens are included. For all the specimens, we observe only

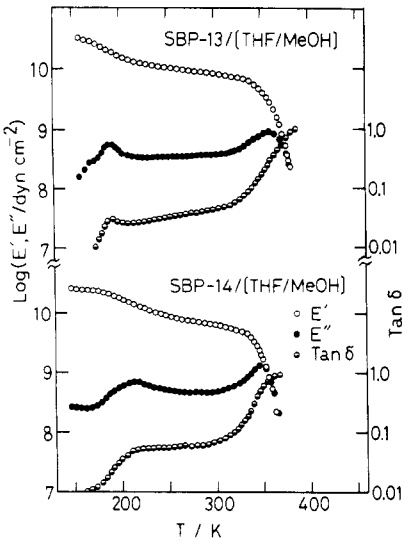

Figure 9. Temperature dependence of E', E'', and tan δ at 110 Hz of SBP-13 and SBP-14 specimens cast from a 9/1 THF/MeOH mixture.

two transitions at about 200 and 370 K, which correspond to the glass transitions of the PB and PS phases, respectively. The values of E' at room temperature decrease with increasing PB content Y.

Figure 8 shows plots of E', E'', and loss tangent δ for SBP-1, -11, and -12 specimens cast from a THF/MeOH (4/1 (v/v)) mixture. For these specimens, we observe three transitions at about 200, 370, and 420 K, which correspond to the glass transitions of the PB, PS, and P4VP phases, respectively. Figure 9 shows similar plots for SBP-13 and -14 cast from a THF/MeOH (9/1 (v/v)) mixture. In contrast to the SBP-1, -11, and -12 specimens exhibiting three transitions, the SBP-13 specimen shows only two transitions at about 200 and 360 K, and the SBP-14 specimen at 210 and 345 K, presumably corresponding to the glass transitions of the PB and PS phases, respectively. The mechanical loss maximum temperature, T_{max}, at the low temperature is slightly higher, while that at the high temperature is lower, than those of the corresponding homopolymers.

Discussion

Composition vs. Domain Shape. For AB-diblock or other simple block copolymers having well-defined molecular architecture, first Meier[21] and later Helfand et al.[22] developed statistical mechanical theories to find the equilibrium domain shape and size as a function of the composition and molecular weight of the block copolymer and the thermodynamic interaction parameters χ_{AB} between the A and B blocks. The domain morphology of the two-component systems was modeled by Molau.[11]

However, in practical cases, many block copolymers do not always exhibit equilibrium morphology but only have one of several possible metastable structures.[12] Meier[21] explained this fact as follows. For example, in a solvent casting process of an AB diblock copolymer from a dilute (transparent) solution, an equilibrium domain structure may be formed when the system reaches a certain critical concentration ϕ_c. Its morphology depends not only on block molecular weights and composition but also on the solvent affinity for the components and the ϕ_c at which the domains are formed (and thus on the interaction parameters χ_{ij} (i, j = A, B, or the solvent, S) of the systems). Even when the solvent is further removed from the system, the domain structure remains in the morphology formed at ϕ_c and may not change its shape to another of a lower

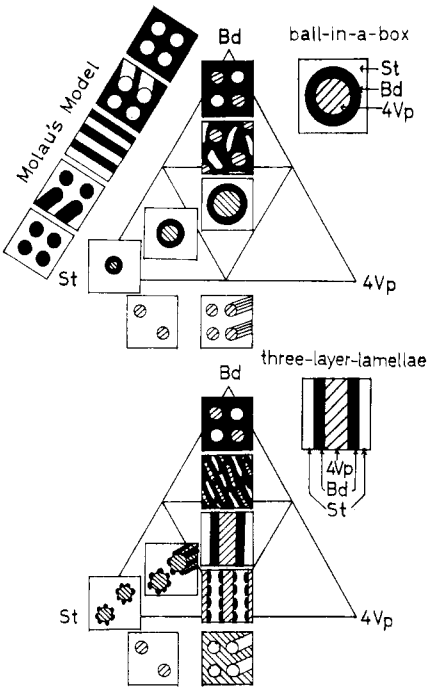

Figure 10. Schematic illustrations of morphological models for the metastable domain structures of SBP, SB, and SP block polymers cast from $CHCl_3$ (above) and from a BA-type solvent (below). The models are arranged at the approximate locations in the composition diagrams.

free energy. Since a domain transformation requires the transport of chains of one component into and through an incompatible medium containing the other component, there is a large kinetic barrier to this transformation. This barrier should become higher and approach that in the bulk as the system is more concentrated by solvent evaporation. Thus, the initially formed structure hardly changes its shape during the rest of the casting process, although some (small) changes in the domain size may take place by the loss of the solvent.

For ABC three-block polymers, the situation must be about the same, although their morphology is much more complicated. On the basis of the results described in this and previous articles,[6-8] the metastable structures in SBP, SB, and SP block polymers may be summarized as schematically shown in Figure 10. Here, the morphology models are classified into two groups according to the type of casting solvent: one cast from $CHCl_3$ and the other cast from BA-system solvents. In each group, the models are displayed in a triangular diagram at the positions approximately corresponding to their composition.

The SBP polymers having X:1:1 composition with high PS content X cast from either type of solvent exhibited a fairly regular morphology, as shown in Figure 10. On the other hand, the SBP polymers having 1:Y:1 composition with high PB content Y exhibited no definite regular domain structures.[6] However, when they were cast from $CHCl_3$, P4VP blocks always formed spherical microdomains. The solvent $CHCl_3$ is poor for P4VP blocks but good for both PS and PB blocks. The solubility parameter difference between PS and PB is about 0.9, while those between PB or PS and P4VP are 2–4 or 1–3, respectively. According to Meier,[21] the kinetic barrier for the morphological transitions may be related to the χ_{AB}, which is in turn related to the square of the solubility parameter difference (and the block molecular weight). This means that the isolated microdomains involving P4VP blocks are most unlikely to undergo any transition accompanying the transport of the P4VP blocks into and through the me-

dium consisting especially of its poor solvent and PB and/or PS blocks. Obviously, casting from $CHCl_3$ causes P4VP blocks to coagulate and form spherical microdomains at an early stage. Such spherical P4VP domains should be fixed in place and remain unchanged throughout the rest of the casting process.

The BA/$CHCl_3$ (9/1) mixture is almost good for any of the components. However, as $CHCl_3$ is lost in an early stage of casting, the solvent consisting mostly of BA becomes poor for PB blocks, moderate for PS, and good for P4VP. On the other hand, the THF/MeOH (4/1) mixture is always poor (or bad) for PB blocks, moderate or poor for PS blocks, but good (or fair) for P4VP blocks, since the solvent composition remains almost unchanged during the entire process of casting.[7] Thus, during the entire stage of casting from a BA/$CHCl_3$ mixture, the solvent is probably distributed rather favorably to the P4VP phase but less favorably to the PB phase. Thus, the SBP polymers with nearly 1:1:1 composition ended up with a "three-layer-lamellar" structure.[6,7] However, when a THF/MeOH mixture was used as the casting solvent, the solvent may be more unevenly distributed among the three components, allowing PB blocks to coagulate first. Therefore, the PB phase formed dotted-line-like domains rather than continuous lamellae.

In the SBP polymers with large PB content Y cast from one of these BA-system solvents, we found that irregular PS and P4VP domains are intermixed with the PB matrix phase. The mid-PB blocks of the SBP polymers probably coagulate in an early stage of casting, entrapping some of the PS and P4VP blocks and preventing them from forming regular domains. On the other hand, the SBP polymers with X:1:1 composition cast from BA-system solvents formed a fairly regular structure, presumably because their gross structure may be determined by the major component PS.

The metastable morphology of SB diblock copolymers cast from $CHCl_3$ happened to resemble Molau's models, as schematically shown on the SB side of the diagram in Figure 10. Many authors[12,23,24] have reported that AB diblock copolymers such as poly(styrene-*b*-isoprene) (SI) and SB diblock copolymers cast from a solvent good for both components usually exhibit a close-to-equilibrium morphology. Hence, the present results for $CHCl_3$-cast SB specimens may be reasonable. We did not examine the morphology of SB cast from BA-system solvents, because these solvents are poor for SB, giving only opaque solutions.

For SP-1 diblock copolymer with 1:1 composition, a phase inversion was induced by the change in casting solvents. In such a block copolymer, the matrix phase always consisted of the component to which the casting solvent was preferentially distributed. This result is consistent with those reported earlier by Grosius et al.[25] for similar SP diblock copolymers.

Block Length vs. Domain Size. According to the theories developed by Meier[21] and Helfand et al.[22] for AB diblock copolymers under the narrow-interface approximation, the identity period D of lamellar structures and the radii R of cylindrical or spherical microdomains are proportional to the $^2/_3$ power of the number-average molecular weights, M_{nt} and M_{nb}, of the whole block polymer and the blocks forming the particular domains, respectively. Hashimoto and Kawai[23,24] tested this dependence for poly(styrene-*b*-isoprene) (SI) and poly(styrene-*b*-butadiene) (SB) diblock copolymers by small-angle X-ray scattering (SAXS).[26] Later, they[27] extended the test to poly(styrene-*b*-(4-vinylbenzyl)dimethylamine-*b*-isoprene) three-block (SAI) polymer of the ABC type synthesized by Fujimoto et al.[4]

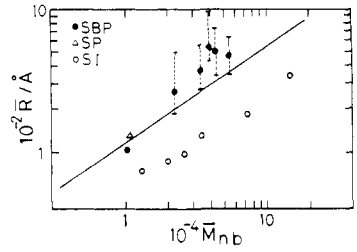

Figure 11. Domain radii R vs. the block molecular weight M_{nb} for SI,[23,24] SP, and SBP block polymers, all having spherical microdomains. The solid line represents the theoretical curve by Helfand[22] for SI systems.

The present SBP specimens cast from different solvents formed metastable structures, which were reproducible but obviously far from their equilibrium states. Also no precise morphology data were obtained, for example, by SAXS. Nevertheless, it might be worthwhile to compare the domain size data for the SBP specimens estimated from the electron micrographs with those of AB diblock and other block polymers obtained by SAXS and of the theoretical predictions[21,22] for AB diblock copolymer systems.

Data on the domain spacings D vs. the total molecular weight, M_{nt}, for SBP-1, -10, and -11 samples cast from BA-type solvents were compared with the SAXS data by Hashimoto and Kawai on SI diblock copolymers[24] and on an SAI three-block polymer.[27] All these specimens had lamellar structures. In spite of the fact that the electron micrographic data on the SBP polymers were rather crude, the SBP data were found to agree fairly well with the theories[21,22] and the SAXS data on SI and SAI block polymers.[24,27]

Figure 11 shows plots of the radii R of the spherical domains vs. the molecular weight M_{nb} of the blocks for SBP polymers and SP block copolymers and those by SAXS on SI diblock copolymers.[23,24] All these specimens exhibited sphere/matrix morphology. Hashimoto and Kawai[23,24] reported that the observed radii R of S domains in I-rich SI diblock copolymers cast from toluene (a good solvent for both PS and PI) were systematically smaller than the theoretical values. They[23,24] explained this discrepancy between their SAXS data and the theoretical predictions as one of the manifestation of metastable structures especially of an isolated sphere/matrix type. In such a specimen, spheres with nonequilibrium sizes are likely to appear, because the equilibrium domain size may be attained only by moving, in this case, the PS blocks in the isolated domains through the PI matrix phase and overcoming the unfavorable enthalpy of mixing of PS and PI blocks.[23,24]

On the other hand, for the SBP polymers cast from $CHCl_3$ the domain size of the P4VP globules is 2–3 times larger than that expected from the block molecular weight M_{nb}. One possible explanation is that the P4VP globules entrap some SBP polymers. This is quite likely to occur, because $CHCl_3$ is a poor solvent for P4VP. Another possibility is that the P4VP blocks take on an extended conformation in the globules. Only a 20–40% increase in the end-to-end distance of the P4VP blocks could explain the discrepancy in question. At present, however, we find no reasonable explanation on why such an chain extension should occur in the spherical microdomains of P4VP blocks, except that the interaction parameter χ_{AB} between P4VP and other blocks is fairly large.

Loss Maximum Temperature vs. Domain Morphology. The SBP polymers exhibit different viscoelastic

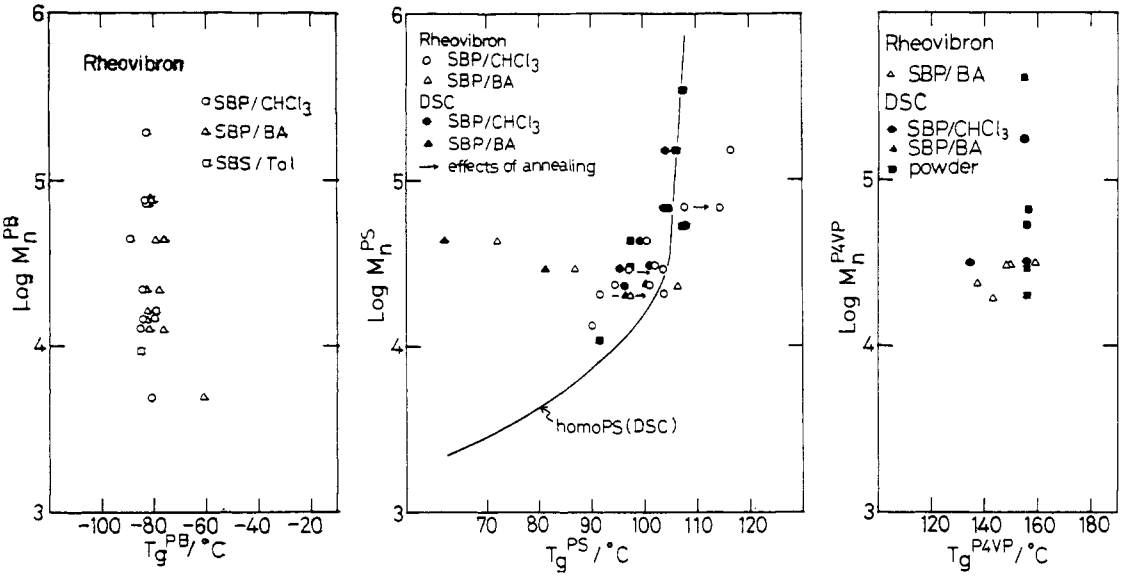

Figure 12. Log (block molecular weight M_{nb}) vs. the loss maximum temperature T_{max} and T_g for PB blocks (left), PS blocks (center), and P4VP blocks (right) in SBP and SBS block polymers cast from various solvents as indicated.

properties,[6,8] corresponding to their unique morphology arising from the difference in casting solvents. Those cast from $CHCl_3$ show only two (viscoelastic) relaxations corresponding to the glass transitions of the PB and PS phases. On the other hand, those cast from a BA-system solvent, except SBP-13 and -14 samples, exhibit three relaxations at about the T_g of the PB, PS, and P4VP phases.

This difference in the viscoelastic properties of $CHCl_3$- and BA-cast specimens of a given SBP sample was successfully explained by applying a finite element method to SBP-1 specimens modeled by a "ball-in-a-box" and a "three-layer-lamellar" structure.[28] The difference is obviously related to the "continuity" of the hard P4VP phase in the specimen. In the former, the P4VP phase forms dispersed spherical domains surrounded by soft PB blocks which connect the P4VP blocks to the PS matrix. On the other hand, in the latter, all three blocks form continuous domains. Therefore, in the specimen having a "ball-in-a-box" structure, the mechanical excitation to the matrix phase may not be transmitted to the P4VP domains but may be absorbed and dissipated in the PB phase. This is also probably the case for BA-cast SBP-13 and -14 samples, which have low P4VP content, and hence, the P4VP domains are not continuous but dispersed even in their BA-cast specimens.

If this interpretation is true, the T_g of the P4VP phase could be determined by a calorimetric method such as DSC or by dielectric spectroscopy, because in these experiments the excitation should be transmitted to the P4VP phase no matter how the PB phase is intervening. Figure 12 summarizes the T_{max} and DSC T_g data for PB, PS, and P4VP blocks as functions of their block molecular weights M_{nb}. As anticipated, the T_g of the P4VP phase could be determined by DSC for all the specimens regardless of the casting solvent used.

Another interesting observation concerning the T_{max} and T_g data is that BA-cast specimens of SBP-2 and -3 with high PB content showed very low T_{max} for the PS and P4VP phases, while that for the PB phase remained almost unchanged. The same BA-cast specimens also showed a similar large decrease in T_g (see Figure 12). However, the decrease in E' at the T_{max} of the PB phase was very small for the BA-cast specimens, as compared to that for the $CHCl_3$-cast specimens.[6,7] These results are obviously associated with a large-scale mixing of the component blocks, because BA (or THF/MeOH) is a rather poor solvent for PB blocks and thus promotes coagulation of PB blocks and entrapment of PS and P4VP blocks, as discussed before.

It should also be noted that the SBP-13 and -14 samples having high PS content cast from a THF/MeOH (9/1 (v/v)) mixture, one of the BA-system solvents, exhibit rather broad transitions at about 210 K and in the region from 350 to 360 K. The former is somewhat higher than that of PB homopolymer, while the latter is lower than that of PS homopolymer. This small shift in T_{max} and also the broadening of the loss peak is probably due to small-scale mixing of the components in the interfacial region, again for the reasons mentioned above. This kind of small shift in T_{max} or T_g could also happen simply by casting the block polymer from its common solvent, because the segregation power between the component blocks is usually less in a common solvent than in a preferential solvent.

The similar large decrease and small shift in T_{max} or T_g found in SI diblock copolymers cast from various solvents were examined by Hashimoto et al.[29] using SAXS and the mechanical-model analysis proposed by Kraus.[30] They concluded that the mixing of the two components at the interfacial region leads to the slight shift in the T_{max} and the broadening of the loss peaks, whereas the large-scale mixing of the components in the domains results in a large decrease in the T_{max} of the hard-segment phase. They called these two phenomena the "domain-boundary mixing" and the "mixing-in-domain" effects, respectively. Obviously, the same interpretation may be made for the present SBP polymers with unequal compositions cast from one of the BA-system solvents.

Acknowledgment. We thank Dr. Koichi Arai for valuable advice on the anionic polymerization experiments and Mr. Kenji Yoshimura, Toray Research Center, for taking excellent electron micrographs. We also thank Mr. Nobuo Donkai, Dr. Takeshi Tanaka-Fukuda, and Professor Hiroshi Inagaki, Institue for Chemical Research, Kyoto University at Uji, for assistance in the molecular characterization experiments on the SBP polymers. The work was supported by the Ministry of Education, Science, and Culture (Mombusho), Japan, under Grant 543026, for which we express our sincere thanks.

References and Notes

(1) Kurihara, M.; Kamachi, M.; Stille, J. K. *J. Polym. Sci., Polym. Chem. Ed.* **1973**, *C26*, 117.

(2) Hsieh, H. L. *J. Appl. Polym. Sci.* **1978**, *22*, 1119.
(3) Koestsier, D. W.; Bantjes, A.; Feijen, J. *J. Polym. Sci., Polym. Chem. Ed.* **1978**, *16*, 511.
(4) Matsushita, Y.; Chosi, H.; Fujimoto, T.; Nagasawa, M. *Macromolecules* **1980**, *13*, 1053.
(5) Riess, G.; Schlienger, M.; Marti, S. *J. Macromol. Sci., Phys.* **1980**, *B17*, 355.
(6) Arai, K.; Kotaka, T.; Kitano, Y.; Yoshimura, K. *Macromolecules* **1980**, *13*, 457, 1670.
(7) Arai, K.; Ueda-Mashima, C.; Kotaka, T.; Yoshimura, K.; Murayama, K. *Polymer*, in press.
(8) Kudose, I. M.S. Dissertation, Department of Macromolecular Science, Osaka University, 1983.
(9) Matsushita, Y.; Yamada, K.; Hattori, T.; Fujimoto, T.; Sawada, Y.; Nagasawa, M.; Matsui, C. *Macromolecules* **1983**, *16*, 10.
(10) Funabashi, H.; Miyamoto, Y.; Isono, Y.; Fujimoto, T.; Matsushita, Y.; Nagasawa, M. *Macromolecules* **1983**, *16*, 1. Isono, Y.; Tanisugi, H.; Endo, K.; Fujimoto, T.; Hasegawa, H.; Hashimoto, T.; Kawai, H. *Macromolecules* **1983**, *16*, 5.
(11) Molau, G. E. "Block Polymers"; Aggarwal, S. L., Ed.; Plenum Press: New York, 1970; p 29.
(12) Sadron, C.; Gallot, B. R. M. *Makromol. Chem.* **1973**, *164*, 301. Gallot, B. R. M. *Adv. Polym. Sci.* **1978**, *29*, 85.
(13) Morton, M.; Fetters, L. J. *Rubber Chem. Technol.* **1975**, *48*, 359.
(14) Fujimoto, T.; Nagasawa, M. "Advanced Techniques for Polymer Synthesis"; Kagakudojin: Kyoto, 1972.
(15) Kamienski, C. W.; Eastham J. F. *J. Org. Chem.* **1969**, *34*, 1116.
(16) Luxton, A. R.; Quig, A.; Delvaux, M.; Fetters, L. J. *Polymer* **1978**, *19*, 1320.
(17) Brandrup, J.; Immergut, E. H., Eds. "Polymer Handbook", 2nd ed.; Wiley: New York, 1975; Chapters III and V.
(18) Morero, D.; Santambroglio, A.; Gianotti, G. *J. Polym. Sci.* **1961**, *51*, 475.
(19) Santee, E. R., Jr.; Malotky, L. O.; Morton, M. *Rubber Chem. Technol.* **1973**, *46*, 1156.
(20) Frosini, V.; de Petris, S. *Chem. Ind. (Milan)* **1967**, *49*, 1178.
(21) Meier, D. J. *J. Polym. Sci.* **1969**, *C26*, 81. Burke, J. J.; Weiss, V., Eds. "Block and Graft Copolymers"; Syracuse University Press: Ithaca, NY, 1973; Chapter 6.
(22) Helfand, E. *Macromolecules* **1975**, *8*, 552. Helfand, E.; Wasserman, Z. R. *Macromolecules* **1976**, *9*, 879. Helfand, E.; Wasserman, Z. R. *Macromolecules* **1978**, *11*, 960.
(23) Hashimoto, T.; Shibayama, M.; Kawai, H. *Macromolecules* **1980**, *13*, 1237. Hashimoto, T.; Fujimura, M.; Kawai, H. *Macromolecules* **1980**, *13*, 1660.
(24) Hashimoto, H.; Fujimura, M.; Hashimoto, T.; Kawai, H. *Macromolecules* **1981**, *14*, 844. Fujimura, M.; Hashimoto, H.; Kurahashi, K.; Hashimoto, T.; Kawai, H. *Macromolecules* **1981**, *14*, 1196.
(25) Grosius, P.; Gallot, Y.; Skoulios, A. *Makromol. Chem.* **1969**, *127*, 94. Grosius, P.; Gallot, Y.; Skoulios, A. *Eur. Polym. J.* **1970**, *6*, 355.
(26) Hashimoto, T.; Shibayama, M.; Fujimura, M.; Kawai, H. *Mem. Fac. Eng., Kyoto Univ.* **1981**, *43* (2), 184.
(27) Shibayama, M.; Hasegawa, H.; Hashimoto, T.; Kawai, H. *Macromolecules* **1982**, *15*, 274.
(28) Watanabe, H.; Kotaka, T. *Polym. J.* **1981**, *13*, 149.
(29) Hashimoto, T.; Tsukahara, Y.; Kawai, H. *Kobunshiyokoshu* **1982**, *31*, 2577. Hashimoto, T.; Tsukahara, Y.; Tachi, K.; Kawai, H. *Kobunshiyokoshu* **1982**, *31*, 2581.
(30) Kraus, G.; Rollman, W. *J. Polym. Sci.* **1976**, *14*, 1133.

Phenomenological Model of the Stress–Strain Behavior of Glassy Polymers

J. Skolnick,*† Dennis Perchak, and Robert Yaris

Department of Chemistry, Washington University, St. Louis, Missouri 63130

Jacob Schaefer

Physical Sciences Center, Monsanto Company, St. Louis, Missouri 63167.
Received January 10, 1984

ABSTRACT: Flow processes in glassy polymers under stress are identified with the orientation of chain segments which are large relative to a bond length but small relative to the chain length. A phenomenological expression is presented for the stress in terms of the strain and an order parameter characterizing the degree of segmental orientation. With this model, physical arguments are presented to describe qualitatively features of a stress–strain experiment including (1) the temperature dependence, (2) the initial time lag, (3) the effects of sudden changes in strain rate, and (4) the relationship between tension and compression.

I. Introduction

The response of a glassy polymer to an imposed stress is an important physical property of the plastic.[1] Of particular importance for the understanding of this behavior is the identification of the molecular processes accompanying the transition from the low-strain, elastic deformation regime to the high-strain, plastic-flow regime of a glassy polymer. To help in this task we present in this paper a phenomenological model of the behavior of a glassy polymer under stress. The model described below is still a long way from a proper theory of stress–strain behavior, primarily because we do not have an adequate mathematical realization of the physical ideas. However, even without the mathematics, we can show that the physical picture emerging from the model rationalizes a variety of experimental results. It is precisely this broad degree of qualitative agreement that convinces us that the physical picture we are presenting is reasonable. It is our hope that by presenting this qualitative picture we will stimulate the work that still needs to be done to obtain an adequate theoretical understanding of the stress–strain behavior of glassy polymers.

The next section presents the model we are proposing along with some discussion of the experimental results that support various aspects of the model. This will be followed in section III by a brief discussion of some of the existing theoretical models of stress–strain behavior. The object of this discussion is to point out why a new approach is necessary to explain the experimental results. We will then show that our model can explain qualitatively a wide variety of additional experimental results.

II. Basic Physical Model

A. Orientation of Chain Segments. The starting point for our model of the stress–strain behavior of glassy

† Alfred P. Sloan Foundation Fellow.

0024-9297/84/2217-2332$01.50/0